Mutant induced pluripotent stem cell lines recapitulate aspects of TDP-43 proteinopathies and reveal cell-specific vulnerability

Bilada Bilican[a,b], Andrea Serio[a,b], Sami J. Barmada[c,d], Agnes Lumi Nishimura[e], Gareth J. Sullivan[b], Monica Carrasco[f], Hemali P. Phatnani[f], Clare A. Puddifoot[g], David Story[a,b], Judy Fletcher[b], In-Hyun Park[h], Brad A. Friedman[i], George Q. Daley[j], David J. A. Wyllie[g], Giles E. Hardingham[g], Ian Wilmut[b], Steven Finkbeiner[c,d], Tom Maniatis[f,1], Christopher E. Shaw[e,1,2], and Siddharthan Chandran[a,b,k,1,2]

[a]Euan MacDonald Centre for Motor Neurone Disease Research, [b]Medical Research Council Centre for Regenerative Medicine, [k]Centre for Neuroregeneration, University of Edinburgh, Edinburgh EH16 4SB, United Kingdom; [e]Institute of Psychiatry, Medical Research Council Centre for Neurodegeneration Research, King's College London, London SE5 8AF, United Kingdom; [g]Centre for Integrative Physiology, University of Edinburgh, Edinburgh EH8 9XD, United Kingdom; [h]Yale Stem Cell Center, Department of Genetics, Yale School of Medicine, New Haven, CT 06520; [f]Department of Biochemistry and Molecular Biophysics, Columbia University, New York, NY 10032; [j]Department of Biological Chemistry and Molecular Pharmacology, Harvard Stem Cell Institute, Harvard Medical School, Boston, MA 02115; [c]Taube-Koret Center, Hellman Program, and Rodenberry Stem Cell Program, Gladstone Institute of Neurological Disease, San Francisco, CA 94158; [d]Departments of Neurology and Physiology, University of California, San Francisco, CA 94143; and [i]Department of Molecular and Cellular Biology, Harvard University, Cambridge, MA 02138

Contributed by Tom Maniatis, February 22, 2012 (sent for review January 10, 2012)

Transactive response DNA-binding (TDP-43) protein is the dominant disease protein in amyotrophic lateral sclerosis (ALS) and a subgroup of frontotemporal lobar degeneration (FTLD-TDP). Identification of mutations in the gene encoding TDP-43 (*TARDBP*) in familial ALS confirms a mechanistic link between misaccumulation of TDP-43 and neurodegeneration and provides an opportunity to study TDP-43 proteinopathies in human neurons generated from patient fibroblasts by using induced pluripotent stem cells (iPSCs). Here, we report the generation of iPSCs that carry the TDP-43 M337V mutation and their differentiation into neurons and functional motor neurons. Mutant neurons had elevated levels of soluble and detergent-resistant TDP-43 protein, decreased survival in longitudinal studies, and increased vulnerability to antagonism of the PI3K pathway. We conclude that expression of physiological levels of TDP-43 in human neurons is sufficient to reveal a mutation-specific cell-autonomous phenotype and strongly supports this approach for the study of disease mechanisms and for drug screening.

disease modeling | reprogramming | motor neuron disease | Lou Gehrig disease

Cytoplasmic accumulation of detergent-resistant transactive response DNA-binding (TDP-43) is a pathological hallmark of both sporadic and inherited FTLD-TDP (a subgroup of frontotemporal lobar degeneration) and ALS [except superoxide dismutase 1 (SOD1) and fused in sarcoma (FUS) cases] and suggests a common pathological mechanism (1–4). Mutations in the gene encoding TDP-43 (*TARDBP*) have been identified in familial and sporadic ALS (5–8). Several in vitro and in vivo models established the toxicity of ALS-associated TDP-43 mutations, although the underlying mechanism is unclear (9, 10). Most cellular and animal models of ALS and FTLD-TDP pathogenesis involve overexpression of TDP-43 in nonneuronal or nonhuman cells and cannot be used to investigate the selective vulnerability of neurons or key molecular events that are unique to human cells. By contrast, induced pluripotent stem cells (iPSCs) (11–14) coupled with defined in vitro differentiation protocols (15–20) offer a model system to investigate disease mechanisms in a more physiological context. Here, we report the pathological effects of endogenous mutant TDP-43 in iPSC-derived human neurons from an ALS patient carrying the M337V mutation.

Results

Generation of iPSCs from TDP-43 M337V Fibroblasts. iPSC lines were established by using cells from a 56-y-old man with ALS who had the TDP-43 M337V mutation (8, 21) and from two healthy controls. Fibroblasts (Fig. 1*A*) were transduced with retroviral vectors encoding the reprogramming factors *OCT4*, *SOX2*, *KLF4*, and *c-MYC* as described in ref. 13. Colonies with compact human ES cell (hESC)-like morphology were expanded, and clonal lines were established for both genotypes (Fig. 1*B*). All iPSCs used in the study exhibited silencing of the four transgenes and activation of endogenous *OCT4*, *SOX2*, and *KLF4* (Fig. S1*A*). All iPSCs expressed the protein markers of pluripotency—OCT4, SOX2, and TRA-1-60 (Fig. 1 *C* and *D* and Fig. S1*B*)—and had comparable levels of *OCT4*, *SOX2*, *c-MYC*, *KLF4*, and *NANOG* expression, as determined by quantitative RT-PCR (qRT-PCR) (Fig. 1*G* and Fig. S1*C*). Pluripotency was confirmed by teratoma formation (Fig. S1*D*) and bisulfite sequencing of the *OCT4* promoter (13) (Fig. 1*F*). The genetic mutation was confirmed by direct sequencing of exon 6 in *TARDBP* in all lines (Fig. 1*E*). All clones were maintained a normal karyotype for more than 40 passages.

TDP-43 M337V Does Not Prevent Differentiation and Functional Maturation of Motor Neurons (MNs). To assess the effects of the TDP-43 M337V mutation on neural differentiation and function, we generated caudalized neuronal populations containing spinal MNs from iPSCs as described previously (21–23). Feeder-free iPSCs were differentiated into neuroectoderm by dual-SMAD signaling inhibition (21) (Fig. 2*A* and Fig. S2*A*). Replating generated >90% NESTIN$^+$ and SOX1$^+$ cells (Fig. 2 *B* and *C*). PAX6$^+$ neuroepithelial cells (Fig. S2*B*) were treated with retinoic acid and purmorphamine to generate *NKX6.1* and OLIG2$^+$ ventral spinal progenitors (Fig. 2*A* and Fig. S2*C*), which differentiated into MNs expressing HB9, β3-tubulin, SMI-32, and choline acetyltransferase (ChAT) (Fig. 2 *D*–*F* and Fig. S2*D*) (23–25). Current–clamp recordings from ChAT$^+$ MNs derived from M337V and control iPSCs revealed tetrodotoxin-sensitive action

Author contributions: B.B., A.S., S.J.B., M.C., H.P.P., B.A.F., G.Q.D., D.J.A.W., G.E.H., I.W., S.F., T.M., C.E.S., and S.C. designed research; B.B., A.S., S.J.B., G.J.S., C.A.P., D.S., J.F., and I.-H.P. performed research; B.B., A.S., S.J.B., A.L.N., G.Q.D., S.F., T.M., and C.E.S. contributed new reagents/analytic tools; B.B., A.S., S.J.B., C.A.P., I.-H.P., B.A.F., and S.C. analyzed data; and B.B., A.S., S.J.B., G.J.S., M.C., H.P.P., D.J.A.W., G.E.H., I.W., S.F., T.M., C.E.S., and S.C. wrote the paper.

The authors declare no conflict of interest.

Freely available online through the PNAS open access option.

[1]To whom correspondence may be addressed. E-mail: tm2472@columbia.edu, christopher.shaw@kcl.ac.uk, or siddharthan.chandran@ed.ac.uk.

[2]C.E.S. and S.C. contributed equally to this work.

This article contains supporting information online at www.pnas.org/lookup/suppl/doi:10.1073/pnas.1202922109/-/DCSupplemental.

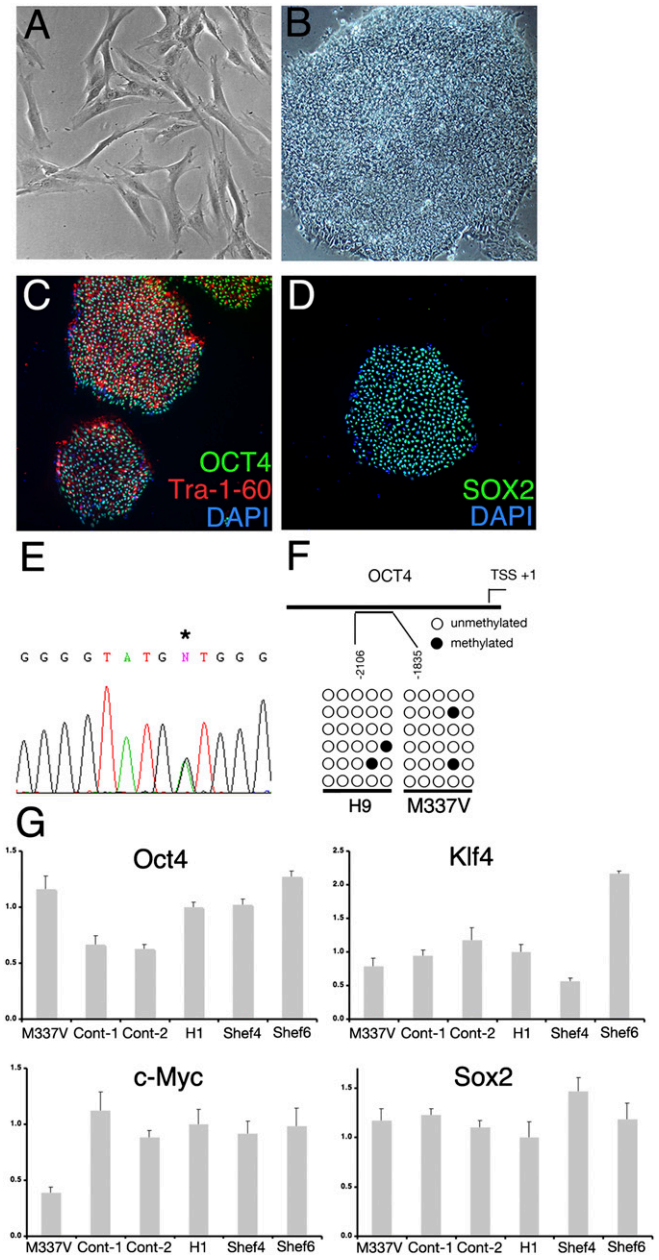

Fig. 1. Establishment of iPSCs from patient fibroblasts. (*A* and *B*) Primary dermal fibroblasts from an ALS patient (*A*) formed tightly packed hESC-like colonies (*B*) after lentiviral reprogramming with OCT4, SOX2, KLF4, and c-MYC. (*C* and *D*) Immunohistochemical characterization of feeder-free patient iPSCs for the pluripotency markers OCT4, Tra-1-60, and SOX2. (*E*) Direct sequencing confirmed the M337V mutation in TDP-43 in patient-derived iPSCs. (*F*) Bisulfite sequencing analysis of the *OCT4* promoter in M337V iPSCs and hESC line H9s. (*G*) qRT-PCR comparison of total expression levels of OCT4, KLF4, c-MYC, and SOX2 in M337V and WT iPSCs and hESC lines H1, Shef4, and Shef6. Values are mean ± SEM. All results are from M337V iPSC clone 2 (M337V-2) except *G* and are representative of iPSC clone M337V-1.

potentials (Fig. 2 *G* and *H*). Whole-cell voltage–clamp recordings revealed functional NMDA, AMPA, and GABA receptors that typify MNs (Fig. S2 *E* and *F*). Mature MN cultures also exhibited spontaneous excitatory postsynaptic currents (EPSCs) that were blocked by 6-cyano-7-nitroquinoxaline-2,3-dione (CNQX) (Fig. 2*I*). Thus, both M337V and control iPSC lines generated phenotypically and functionally comparable MNs (26–28).

M337V Increases Soluble and Detergent-Resistant TDP-43 Protein Levels. A defining biochemical feature of diseased ALS and FTLD-TDP neural tissue is the accumulation of detergent-resistant ~43-kDa and C-terminal fragments of TDP-43 (29). We next examined the biochemical profile of TDP-43 in undifferentiated iPSCs. As determined by qRT-PCR, M337V and control iPSC lines expressed similar levels of *TARDBP*, the pluripotency markers *TERT* and *REX1*, and *histone deacetylase 6* (*HDAC6*) mRNA (Fig. 3*A*), the latter of which is regulated by TDP-43 (30). Western blotting revealed that two independent M337V iPSC clones had higher levels of full-length TDP-43 in the soluble fraction and C-terminal TDP-43 fragments in the detergent-resistant fraction than controls (Fig. 3*B*). Importantly, TDP-43 fragmentation was not associated with conventional indices of apoptosis [cleaved poly(ADP-ribose) polymerase (PARP) (Fig. 3*B*) and annexin V/propidium iodide profiling (Fig. 3*C*)] (31–33).

Before establishing the biochemical profile of TDP-43 in MN-containing neuronal populations, we first verified that MN cultures derived from M337V and control 2 (Cont-2) had comparable expression levels of *TARDBP*, *HB9*, *ChAT*, and *HDAC6* as determined by qRT-PCR analysis (Fig. S3*A*). Furthermore, MN cultures derived from both M337V and controls showed similar percentages of SMI-32$^+$ cells by quantitative immunohistochemistry (Fig. S3*B*), altogether indicating comparable differentiation potential and composition of MN cultures at the point of assay. Immunoblot analysis revealed that M337V MN cultures from two independent clones had up to fourfold higher levels of soluble and detergent-resistant TDP-43 than Cont-2 MN cultures (Fig. 4 *A* and *B*). Difference in TDP-43 levels in MN-containing populations was also evident with Cont-1 MN cultures (see control lanes in Figs. S3*D* and S5*B*). To determine whether this observation was independent of neuronal cell type and differentiation protocol, we generated caudalized neuronal populations that did not contain MNs and compared the amount of TDP-43 in cultures derived from mutant or control iPSCs (Fig. S4 *A* and *B*). Again, M337V neurons had higher levels of soluble (2.6 ± 0.46 vs. 1.0 ± 0.13) and insoluble TDP-43 than controls (Fig. S4 *C* and *D*).

We next investigated the subcellular distribution of TDP-43. Densitometric analysis revealed that strongly SMI-32$^+$ neurons had significantly higher levels of nuclear TDP-43 than SMI-32$^-$ cells (118.89% ± 2.6% vs. 100% ± 2.9%, $P < 0.001$) (Fig. 4). However, the predominant nuclear localization of TDP-43 did not differ in M337V and control lines (Fig. S4*C*). Subtle granular cytoplasmic staining was also detected in SMI-32$^+$ and ChAT$^+$ M337V neurons (Fig. 4 *E* and *F* and Fig. S4 *E* and *F*).

TDP-43 M337V Mutation Confers Selective Cellular Vulnerability to MNs. We next analyzed the survival of M337V and control MNs under basal conditions by longitudinal fluorescence microscopy. To specifically focus on MNs, we transfected M337V and control cultures with a plasmid encoding enhanced GFP under the control of the MN-specific Hb9 promoter described previously (HB9::GFP; Fig. 5*A*) (34). Quantification of GFP$^+$ neurons per well confirmed no difference between M337V and control MN cultures (Fig. S5*A*). Automated fluorescence microscopy, a technique that can image thousands of fluorescently labeled neurons for extended periods of time, was then used to track individual neurons and determine their time of death. Neuronal death was marked by abrupt loss of fluorescence or dissolution of the cell itself, criteria that have proved equally as sensitive as traditional markers of cell death (35, 36). Kaplan–Meier survival analysis was used to plot cumulative hazard curves depicting the risk of death for MNs derived from M337V and control iPSCs (Fig. 5*B*). The relative risk associated with the M337V mutation was calculated by Cox proportional hazards

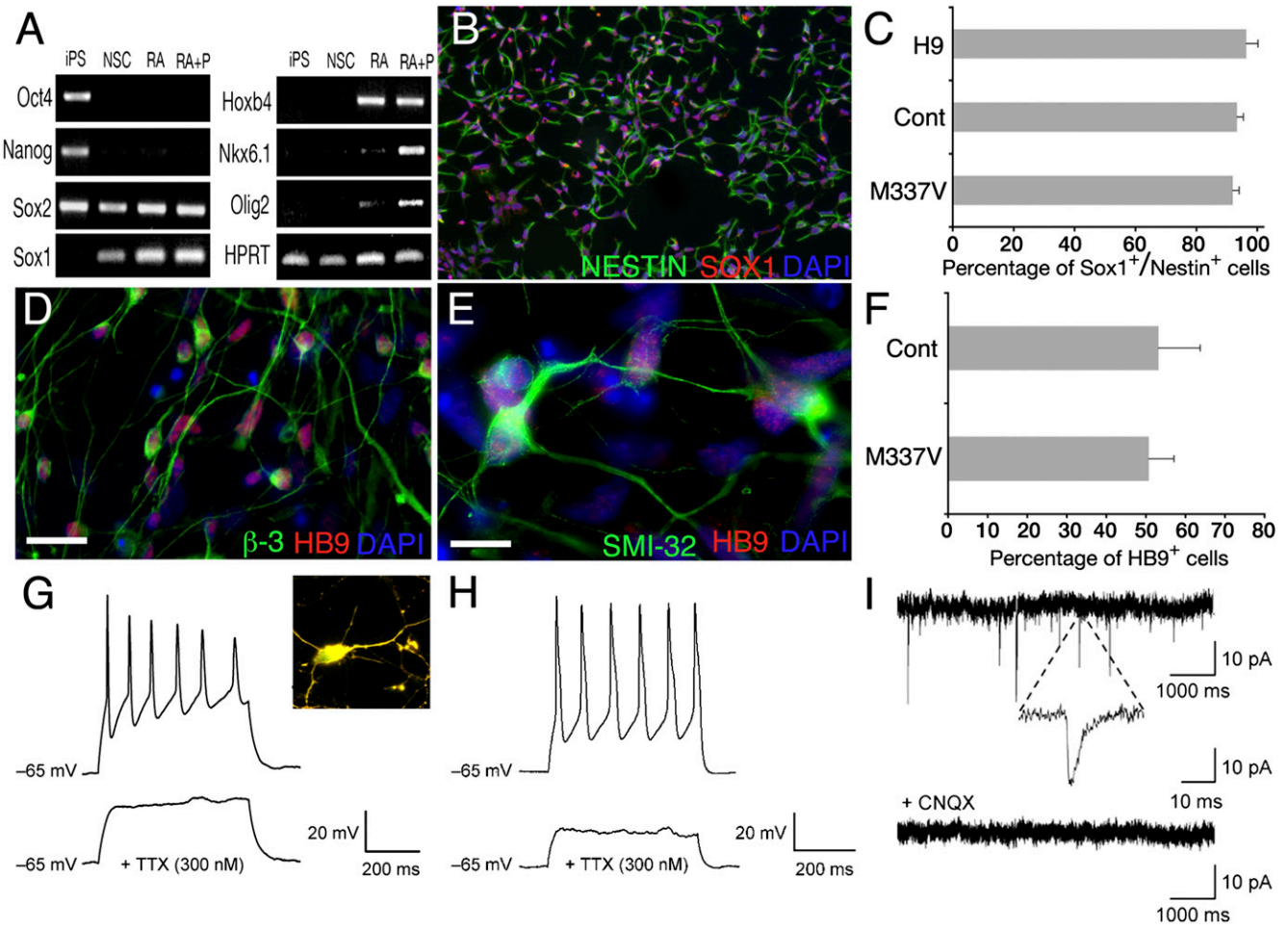

Fig. 2. TDP-43 M337V and control iPSCs can be differentiated into functional MNs. iPSCs or hESCs were directed toward the neuroectodermal lineage by dual-SMAD signaling inhibition in feeder-free, adherent culture conditions. (*A*) M337V iPSCs down-regulate *OCT4* and *NANOG* expression in response to neuralization and up-regulate the lineage-specific genes *SOX1*, *HOXB4*, *NKX6.1*, and *OLIG2* in a temporal order after sequential application of MN patterning factors retinoic acid (RA) and purmorphamine (P). (*B*) Neural differentiation was assessed by quantitative immunohistochemical costaining for Nestin and Sox1 after replating. (*C*) M337V and control iPSCs and H9 hESCs showed similar efficiency in neural differentiation. (*D* and *E*) At 4–6 wk of maturation, iPSC-derived MN progenitors plated on laminin/fibronectin express HB9 and β3-tubulin (*D*) and HB9 and SMI-32 (*E*). (*F*) M337V and control iPSC-derived neural stem cells (NSCs) generated MNs with equal efficiency, as assessed by quantitative immunohistochemistry for HB9. (*G* and *H*) Current–clamp traces showed tetrodotoxin (TTX)-sensitive action potentials in response to injection of depolarizing current in M337V (*G*) and WT (*H*) MNs. (*G Inset*) ChAT and LcY double-positive neuron from which recording is performed. (*I*) Sample traces of spontaneous miniature EPSCs recorded from an M337V culture. All miniature EPSC events were blocked with CNQX. All data are from M337V-2 and Cont-2 iPSCs. Values are mean ± SEM (n = 3). (Scale bars: 10 μm.)

analysis, demonstrating a hazard ratio of 2.76, indicative of a 276% increase in the risk of death in M337V compared with control MNs.

We next determined whether the M337V mutation increased neuronal vulnerability to antagonism of key signaling pathways necessary for neuronal survival (37). MN-containing cultures were treated with U0126, a selective inhibitor of MAPK signaling; LY294002, a selective inhibitor of PI3K; or tunicamycin, an endoplasmic reticulum stressor. After 48 h of treatment, neuronal death was measured by lactate dehydrogenase (LDH) release. M337V and control MN cultures did not differ in their response to MAPK inhibition or tunicamycin (Fig. S5 *C* and *D*). However, M337V mutant lines 1 and 2 were significantly more vulnerable than controls were to LY294002 (Fig. 5*C*), suggesting an intrinsic susceptibility to PI3K inhibition in neurons derived from M337V iPSCs.

Discussion

This paper describes an iPSC model of a TDP-43 proteinopathy in human MNs derived from a patient carrying a pathogenic TDP-43 mutation. Detailed cell-lineage and functional studies showed that the TDP-43 M337V mutation does not affect the functional maturation of neurons, including MNs. However, neurons carrying the mutation had increased levels of soluble and detergent-resistant TDP-43 and reduced survival under basal conditions, suggesting an inherent vulnerability. Mutant neurons were also more susceptible than control neurons to inhibition of PI3K, an essential signaling pathway in neurons (38). Thus, the mutant cells recapitulate key aspects of TDP-43 proteinopathies in vitro, including cell-autonomous neuronal degeneration and the accumulation of insoluble TDP-43. This model will facilitate mechanistic studies, the identification of therapeutic targets, and eventually the development of treatments for ALS and FTLD-TDP.

TDP-43 is intrinsically prone to aggregation, and ALS-linked mutations increase its toxicity, tendency to aggregate, and mislocalization to the cytoplasm (1, 3, 29, 39, 40). Although TDP-43 M337V and control neurons expressed equivalent levels of *TARDBP* mRNA, the mutant cells had significantly higher levels of soluble and detergent-resistant TDP-43. Previously, increased

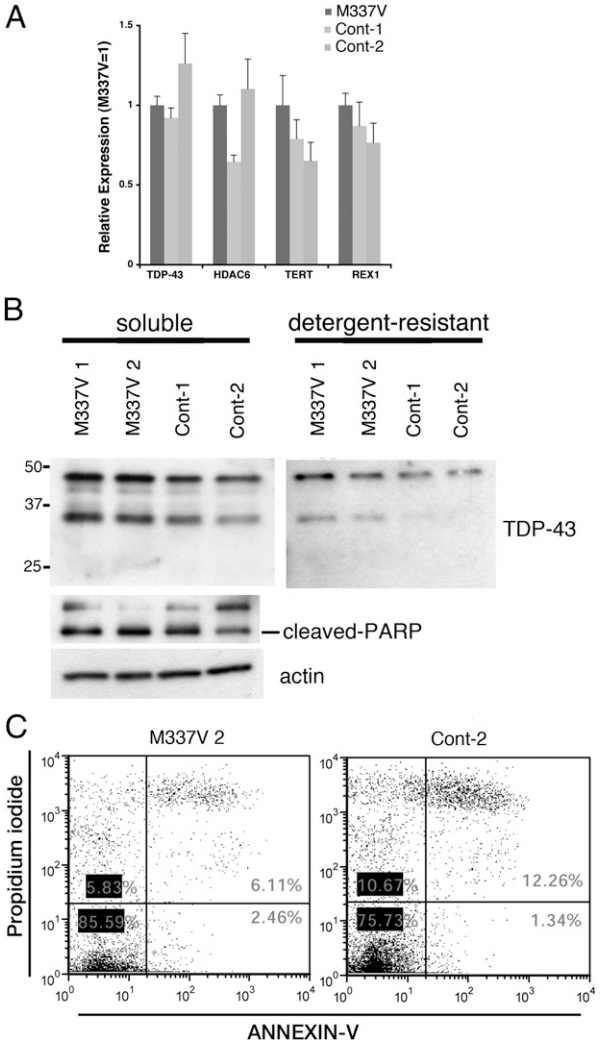

Fig. 3. M337V iPSCs display biochemical features of TDP-43 misaccumulation. (*A*) M337V and control iPSCs express similar levels of *TDP-43*, *REX1*, *TERT*, and *HDAC6*, as determined by qRT-PCR. (*B*) Immunoblots of the detergent-soluble and -insoluble fractions from feeder-free iPSC lysates. TDP-43 fragments of ~35 kDa are enriched in the detergent-resistant fraction of the M337V iPSC lysates. Soluble or insoluble TDP-43 levels do not correlate with cleaved PARP. β-Actin served as a loading control. (*C*) Representative annexin V/propidium iodide staining by flow cytometry. The percentages of cells negative for both annexin V and propidium iodide were similar in M337V-2 (85.6%) and Cont-2 (75.3%) iPSCs, suggesting comparable levels of cell death under basal conditions.

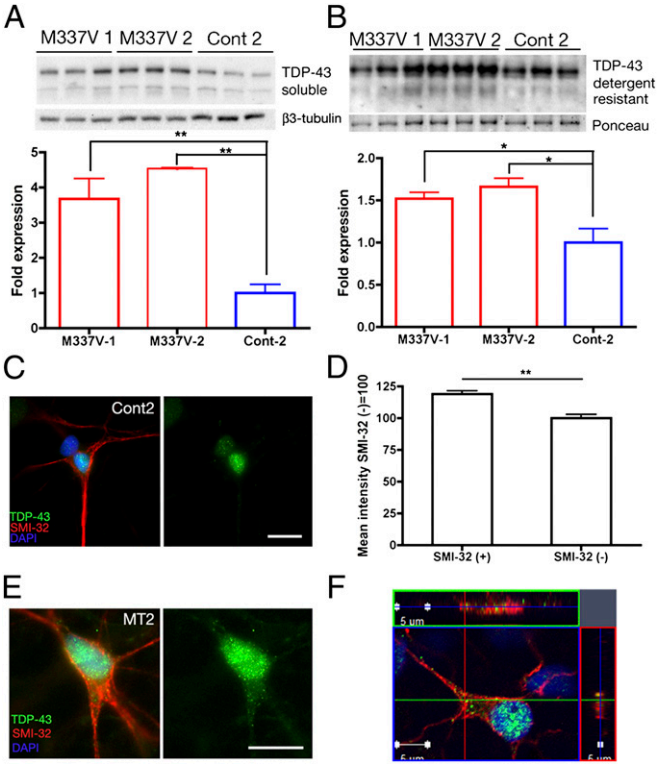

Fig. 4. M337V neurons have higher levels of soluble and detergent-resistant TDP-43. (*A* and *B*) Western blot analysis of M337V-1, M337V-2, and Cont-2 MN-containing cultures. Three independent extractions are shown for each cell line. β3-Tubulin was the loading control for soluble fractions (*A*), and Ponceau S reversible membrane staining (51) was the loading control for detergent-resistant fractions (*B*). Semiquantitative analyses of band signal intensity was accomplished by using ImageJ. (*A*) Levels of soluble TDP-43 normalized to β3-tubulin, Cont-2 set to 1: M337V-1 = 3.67 ± 0.58; M337V-2 = 4.54 ± 0.01; Cont-2 = 1.0 ± 0.24. M337V-1 vs. M337V-2, not significant; M337V-1 vs. Cont-2, $P = 0.013$; M337V-2 vs. Cont-2, $P < 0.001$, $n = 3$ independent extractions. (*B*) Levels of detergent-resistant TDP-43 normalized to Ponceau S, Cont-2 set to 1: M337V-1 = 1.52 ± 0.08; M337V-2= 1.67 ± 0.10; Cont-2 = 1.0 ± 0.16. M337V-1 vs. M337V-2, not significant; M337V-1 vs. Cont-2, $P = 0.04$; M337V-2 vs. Cont-2, $P < 0.03$, $n = 3$ independent extractions. Values are mean ± SEM. Data were analyzed by one-way ANOVA and post hoc Tukey test. (*C* and *D*) Immunofluorescence analysis of nuclear TDP-43 in SMI-32$^+$ and SMI-32$^-$ cells. Cont-2 SMI-32$^+$ (118.89% ± 2.6%) vs. SMI-32$^-$ (100% ± 2.9%), $P < 0.001$, $n = 40$ cells for each group. (*E*) M337V iPSC-derived SMI-32$^+$ MNs displayed predominantly nuclear TDP-43 localization with granular staining present in soma and neurites. (*F*) Orthogonal views through one TDP-43 M337V SMI-32$^+$ cell demonstrating localization of TDP-43 (green), SMI-32 (red), and DAPI (blue). (Scale bars: 10 μm.)

stability of mutant TDP-43 proteins had only been observed in isogenic transformed cell lines (41). Our findings suggest that differences in TDP-43 protein levels result from a posttranslational mechanism rather than from transcriptional differences. In addition, the mutant proteins do not appear to interfere with the proposed autoregulatory feedback mechanism proposed for the control of TDP-43 mRNA levels (42, 43). The dominant missense mutations located in the C-terminal domain of TDP-43 might inhibit the turnover of the mutant protein or constrain protein quality-control pathways.

Despite the higher levels of TDP-43 in M337V neurons detected biochemically, we did not see more nuclear TDP-43 than in controls, as determined by immunofluorescence densitometry. However, SMI-32$^+$ neurons had higher levels of nuclear TDP-43 in vitro, indicating that TDP-43 protein levels can differ between neuronal subtypes. In addition, punctate TDP-43 staining in the soma and cell processes was a consistent finding. This staining pattern is compatible with the involvement of TDP-43 in nucleocytoplasmic shuttling of RNA, the association of TDP-43 with RNA granules in somatodendrites, and the presence of TDP-43 in the microsome fraction of brainstem samples, suggesting active transport of TDP-43 along the axons (44–47).

Cellular and transgenic models of TDP-43 expression established that elevated levels of WT and mutant TDP-43 can be toxic and that levels of cytoplasmic, rather than nuclear, TDP-43 correlate with cellular toxicity (9, 10, 48). As shown by longitudinal fluorescence microscopy of live MNs, the risk of death was significantly increased by the M337V mutation, suggesting an inherent cell-autonomous toxicity of the mutation in MNs. Neuronal health and function are regulated by multiple signals, including brain-derived neurotrophic factor (BDNF), glial cell-derived neurotrophic factor, and other trophic factors that

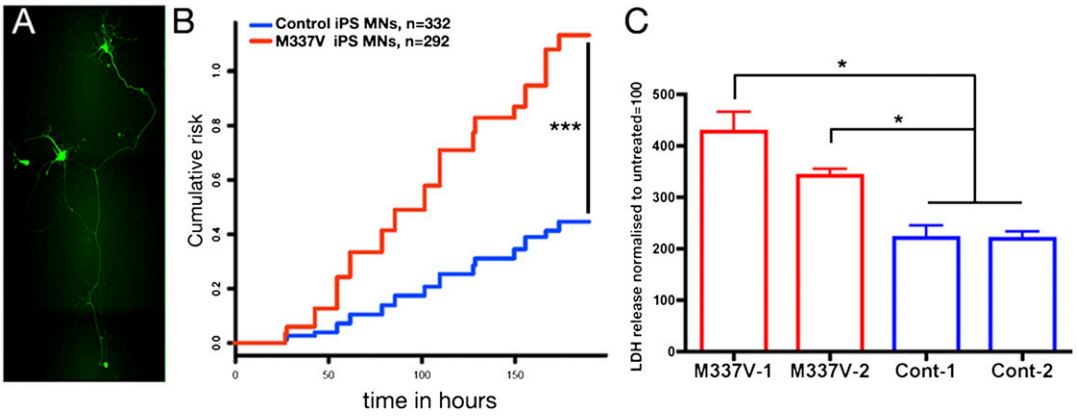

Fig. 5. M337V TDP-43 neurons display selective vulnerability. (*A*) Representative image of an HB9::GFP^{+} neuron used in real-time survival analysis. (*B*) Real-time survival analysis of M337V-1, M337V-2, Cont-1, and Cont-2 MN-containing cultures showing cumulative risk of death of HB9::GFP-transfected neurons. Pooled data from three independent differentiation experiments are shown ($P < 0.001$ between mutant and control groups, log-rank test). (*C*) Cytotoxicity in MN cultures derived from M337V and control iPSCs after treatment with LY294002 (40 μM) for 48 h. A total of 20,000 MN precursors per well were plated in a 96-well format and allowed to differentiate for 4 wk before treatments were started. Fluorescent LDH release measured with a FLUOstar OPTIMA plate reader served as a measure of cytotoxicity. Released LDH was normalized to total LDH for each well, and mock-treated samples were set to 100%. Percentage cytotoxicity for each treatment was determined as a factor of mock treatment for each cell line. Values are mean ± SEM. Data were analyzed by one-way ANOVA and post hoc Tukey test. *$P < 0.05$; M337V-1 vs. M337V-2, not significant; $n = 3$ independent experiments.

signal through receptor tyrosine kinases (37). We demonstrated that M337V neurons were more sensitive to PI3K inhibition than control neurons were but showed no difference in vulnerability to inhibitors of the MAPK pathway or induction of endoplasmic reticulum stress through tunicamycin. Thus, the M337V mutation confers a specific susceptibility to PI3K inhibition, highlighting the importance of trophic factor-mediated signaling in the survival of human MNs. Even though most neurotrophic factors rely on both MAPK/ERK and PI3K/AKT pathways for signal transduction, the contribution of these pathways to cell survival depends on the neuronal subtype and the combination of trophic factors (38). For instance, BDNF-induced MN survival requires the PI3K pathway (49), whereas retinal ganglion cells rely on both the PI3K and MAPK pathways in BDNF-dependent survival (50). Future studies involving the in vitro model that we established herein will focus on the contribution of different neurotrophic factors to the survival of TDP-43 M337V neurons.

In summary, our findings show that patient-derived TDP-43 M337V neurons recapitulate key biochemical aspects of TDP-43 proteinopathies and provide evidence that the M337V mutation in TDP-43 is toxic to iPSC-derived MNs, rendering them particularly susceptible to antagonism of PI3K signaling. Although this study was limited to a single patient line with subclones and controls, we identified a disease-specific phenotype in TDP-43 iPSC lines. Such lines will be useful for exploring the pathogenic mechanisms of other TDP-43 mutations and of different ALS-causing mutations under basal and stress paradigms. Finally, our findings demonstrate the utility of patient-specific iPSC lines in modeling the molecular pathogenesis of adult neurodegenerative disorders.

Materials and Methods

Generation of Human iPSCs. Fibroblasts from a normal male (56 y old; CRL-2465; ATCC), a normal female (40 y old; CRL-2524; ATCC), and from a 56-y-old male carrying the M337V TDP-43 mutation were reprogrammed as previously described (13). Details of iPSC characterization are provided in *SI Materials and Methods*.

Cell Culture. Human iPSC and hESC lines were maintained long term on CF-1 irradiated mouse embryonic fibroblasts, with KO-DMEM (Invitrogen) supplemented with 20% Knockout Serum Replacement (Invitrogen), 10 ng/mL basic FGF2 (PeproTech), 1 mM L-glutamine (Invitrogen), 100 mM 2-mercaptoethanol (Invitrogen), 1% penicillin/streptomycin (Invitrogen), and 1% nonessential amino acids. For the neural conversion, the cells were transitioned to feeder-free culture conditions in MTESR1 media (Stem Cell Technologies) and passaged three times before use. Details of neuronal differentiation and characterization are provided in *SI Materials and Methods*.

Primers and Antibodies. TaqMan and SYBR Green primer sequences are provided in Tables S1 and S2, respectively. Primary antibodies used are listed in Table S3.

ACKNOWLEDGMENTS. We thank Dr. Stephen Goldman for the generous gift of the HB9::GFP plasmid. This work was made possible with support from the Euan MacDonald Centre (S.C.), the Fidelity Foundation (S.C.), the Motor Neurone Disease Association (S.C., T.M., and C.E.S.), the Medical Research Council (C.E.S. and G.E.H.), the Wellcome Trust (G.E.H. and C.E.S.), the Heaton-Ellis Trust (C.E.S.), the BBSRC (C.A.P.), the ALS Association (S.F.), the Rodenberry Stem Cell Program (S.F.), the Hellman Family Foundation Program for Alzheimer's Disease Research (S.F.), the National Institutes of Neurological Disease and Stroke (S.J.B. and S.F.), and the National Institutes on Aging (S.F.).

1. Neumann M, et al. (2006) Ubiquitinated TDP-43 in frontotemporal lobar degeneration and amyotrophic lateral sclerosis. *Science* 314(5796):130–133.
2. Higashi S, et al. (2007) Concurrence of TDP-43, tau and α-synuclein pathology in brains of Alzheimer's disease and dementia with Lewy bodies. *Brain Res* 1184:284–294.
3. Arai T, et al. (2006) TDP-43 is a component of ubiquitin-positive tau-negative inclusions in frontotemporal lobar degeneration and amyotrophic lateral sclerosis. *Biochem Biophys Res Commun* 351:602–611.
4. Uryu K, et al. (2008) Concomitant TAR-DNA-binding protein 43 pathology is present in Alzheimer disease and corticobasal degeneration but not in other tauopathies. *J Neuropathol Exp Neurol* 67:555–564.
5. Yokoseki A, et al. (2008) TDP-43 mutation in familial amyotrophic lateral sclerosis. *Ann Neurol* 63:538–542.
6. Gitcho MA, et al. (2008) TDP-43 A315T mutation in familial motor neuron disease. *Ann Neurol* 63:535–538.
7. Van Deerlin VM, et al. (2008) *TARDBP* mutations in amyotrophic lateral sclerosis with TDP-43 neuropathology: A genetic and histopathological analysis. *Lancet Neurol* 7: 409–416.
8. Sreedharan J, et al. (2008) TDP-43 mutations in familial and sporadic amyotrophic lateral sclerosis. *Science* 319:1668–1672.
9. Wegorzewska I, Baloh RH (2011) TDP-43-based animal models of neurodegeneration: New insights into ALS pathology and pathophysiology. *Neurodegener Dis* 8(9):262–274.
10. Lagier-Tourenne C, Polymenidou M, Cleveland DW (2010) TDP-43 and FUS/TLS: Emerging roles in RNA processing and neurodegeneration. *Hum Mol Genet* 19(R1):R46–R64.
11. Takahashi K, et al. (2007) Induction of pluripotent stem cells from adult human fibroblasts by defined factors. *Cell* 131:861–872.

12. Yu J, et al. (2007) Induced pluripotent stem cell lines derived from human somatic cells. *Science* 318:1917–1920.
13. Park IH, et al. (2008) Reprogramming of human somatic cells to pluripotency with defined factors. *Nature* 451(7175):141–146.
14. Lowry WE, et al. (2008) Generation of human induced pluripotent stem cells from dermal fibroblasts. *Proc Natl Acad Sci USA* 105:2883–2888.
15. Liu Y, Zhang SC (2010) Human stem cells as a model of motoneuron development and diseases. *Ann N Y Acad Sci* 1198:192–200.
16. Lee G, et al. (2009) Modelling pathogenesis and treatment of familial dysautonomia using patient-specific iPSCs. *Nature* 461:402–406.
17. Dimos JT, et al. (2008) Induced pluripotent stem cells generated from patients with ALS can be differentiated into motor neurons. *Science* 321:1218–1221.
18. Ebert AD, et al. (2009) Induced pluripotent stem cells from a spinal muscular atrophy patient. *Nature* 457(7227):277–280.
19. Nguyen HN, et al. (2011) LRRK2 mutant iPSC-derived DA neurons demonstrate increased susceptibility to oxidative stress. *Cell Stem Cell* 8(3):267–280.
20. Carvajal-Vergara X, et al. (2010) Patient-specific induced pluripotent stem-cell-derived models of LEOPARD syndrome. *Nature* 465:808–812.
21. Chambers SM, et al. (2009) Highly efficient neural conversion of human ES and iPS cells by dual inhibition of SMAD signaling. *Nat Biotechnol* 27(3):275–280.
22. Li XJ, et al. (2008) Directed differentiation of ventral spinal progenitors and motor neurons from human embryonic stem cells by small molecules. *Stem Cells* 26:886–893.
23. Wichterle H, Lieberam I, Porter JA, Jessell TM (2002) Directed differentiation of embryonic stem cells into motor neurons. *Cell* 110:385–397.
24. Tsang YM, Chiong F, Kuznetsov D, Kasarskis E, Geula C (2000) Motor neurons are rich in non-phosphorylated neurofilaments: Cross-species comparison and alterations in ALS. *Brain Res* 861(1):45–58.
25. Carriedo SG, Yin HZ, Weiss JH (1996) Motor neurons are selectively vulnerable to AMPA/kainate receptor-mediated injury in vitro. *J Neurosci* 16:4069–4079.
26. Johnson MA, Weick JP, Pearce RA, Zhang SC (2007) Functional neural development from human embryonic stem cells: Accelerated synaptic activity via astrocyte coculture. *J Neurosci* 27:3069–3077.
27. Wada T, et al. (2009) Highly efficient differentiation and enrichment of spinal motor neurons derived from human and monkey embryonic stem cells. *PLoS ONE* 4:e6722.
28. Hu BY, et al. (2010) Neural differentiation of human induced pluripotent stem cells follows developmental principles but with variable potency. *Proc Natl Acad Sci USA* 107:4335–4340.
29. Kwong LK, Uryu K, Trojanowski JQ, Lee VM (2008) TDP-43 proteinopathies: Neurodegenerative protein misfolding diseases without amyloidosis. *Neurosignals* 16(1): 41–51.
30. Fiesel FC, et al. (2010) Knockdown of transactive response DNA-binding protein (TDP-43) downregulates histone deacetylase 6. *EMBO J* 29(1):209–221.
31. Stangl K, et al. (2002) Inhibition of the ubiquitin-proteasome pathway induces differential heat-shock protein response in cardiomyocytes and renders early cardiac protection. *Biochem Biophys Res Commun* 291:542–549.
32. Bush KT, Goldberg AL, Nigam SK (1997) Proteasome inhibition leads to a heat-shock response, induction of endoplasmic reticulum chaperones, and thermotolerance. *J Biol Chem* 272:9086–9092.
33. Kawazoe Y, Nakai A, Tanabe M, Nagata K (1998) Proteasome inhibition leads to the activation of all members of the heat-shock-factor family. *Eur J Biochem* 255:356–362.
34. Singh Roy N, et al. (2005) Enhancer-specified GFP-based FACS purification of human spinal motor neurons from embryonic stem cells. *Exp Neurol* 196(2):224–234.
35. Arrasate M, Mitra S, Schweitzer ES, Segal MR, Finkbeiner S (2004) Inclusion body formation reduces levels of mutant huntingtin and the risk of neuronal death. *Nature* 431:805–810.
36. Arrasate M, Finkbeiner S (2005) Automated microscope system for determining factors that predict neuronal fate. *Proc Natl Acad Sci USA* 102:3840–3845.
37. Cui Q (2006) Actions of neurotrophic factors and their signaling pathways in neuronal survival and axonal regeneration. *Mol Neurobiol* 33(2):155–179.
38. Brunet A, Datta SR, Greenberg ME (2001) Transcription-dependent and -independent control of neuronal survival by the PI3K-Akt signaling pathway. *Curr Opin Neurobiol* 11:297–305.
39. Rutherford NJ, et al. (2008) Novel mutations in *TARDBP* (TDP-43) in patients with familial amyotrophic lateral sclerosis. *PLoS Genet* 4:e1000193.
40. Mackenzie IR, et al. (2009) Nomenclature for neuropathologic subtypes of frontotemporal lobar degeneration: Consensus recommendations. *Acta Neuropathol* 117(1):15–18.
41. Ling SC, et al. (2010) ALS-associated mutations in TDP-43 increase its stability and promote TDP-43 complexes with FUS/TLS. *Proc Natl Acad Sci USA* 107:13318–13323.
42. Polymenidou M, et al. (2011) Long pre-mRNA depletion and RNA missplicing contribute to neuronal vulnerability from loss of TDP-43. *Nat Neurosci* 14:459–468.
43. Ayala YM, et al. (2011) TDP-43 regulates its mRNA levels through a negative feedback loop. *EMBO J* 30(2):277–288.
44. Sato T, et al. (2009) Axonal ligation induces transient redistribution of TDP-43 in brainstem motor neurons. *Neuroscience* 164(4):1565–1578.
45. Elvira G, et al. (2006) Characterization of an RNA granule from developing brain. *Mol Cell Proteomics* 5:635–651.
46. Wang IF, Wu LS, Chang HY, Shen CK (2008) TDP-43, the signature protein of FTLD-U, is a neuronal activity-responsive factor. *J Neurochem* 105:797–806.
47. Braak H, Ludolph A, Thal DR, Del Tredici K (2010) Amyotrophic lateral sclerosis: Dash-like accumulation of phosphorylated TDP-43 in somatodendritic and axonal compartments of somatomotor neurons of the lower brainstem and spinal cord. *Acta Neuropathol* 120(1):67–74.
48. Barmada SJ, et al. (2010) Cytoplasmic mislocalization of TDP-43 is toxic to neurons and enhanced by a mutation associated with familial amyotrophic lateral sclerosis. *J Neurosci* 30:639–649.
49. Dolcet X, Egea J, Soler RM, Martin-Zanca D, Comella JX (1999) Activation of phosphatidylinositol 3-kinase, but not extracellular-regulated kinases, is necessary to mediate brain-derived neurotrophic factor-induced motoneuron survival. *J Neurochem* 73:521–531.
50. Nakazawa T, Tamai M, Mori N (2002) Brain-derived neurotrophic factor prevents axotomized retinal ganglion cell death through MAPK and PI3K signaling pathways. *Invest Ophthalmol Vis Sci* 43:3319–3326.
51. Gozal YM, et al. (2009) Proteomics analysis reveals novel components in the detergent-insoluble subproteome in Alzheimer's disease. *J Proteome Res* 8:5069–5079.